Comparison of System Identification Methods Using Ambient Bridge Test Data

P. Andersen & R. Brincker
Department of Building Technology and Structural Engineering, Aalborg University
Sohngaardsholmsvej 57, DK-9000 Aalborg, Denmark

B. Peeters & G. De Roeck
Department of Civil Engineering, Katholieke Universiteit Leuven
W. De Croylaan 2, B-3001 Heverlee, Belgium

L. Hermans
LMS International
Interleuvenlaan 68, B-3001 Leuven, Belgium

C. Krämer,
EMPA, Swiss Federal Laboratories for Material Testing and Research
Ueberlandstrasse 129. CH-8600 Duebendorf, Switzerland

ABSTRACT

In this paper the performance of four different system identification methods is compared using operational data obtained from an ambient vibration test of the Swiss Z24 highway bridge. The four methods are the frequency domain based peak-picking methods, the polyreference LSCE method, the stochastic subspace method for estimation of state space systems and the prediction error method for estimation of Auto-Regressive Moving Average Vector models. It is not the intention to elect a winner among the four methods, but more to emphasize the different advantages of each of the methods.

NOMECLATURE

y_k	Vector of measured output.
R_k	Correlation function between outputs.
Δt	Sampling interval.
λ_i	Discrete-time system pole.
μ_i	Continuous-time system pole.
$E[\bullet]$	Expectation operator.
ψ_i	Mode shape vector.
L_i	Vector of multipliers.
A	State (transition) matrix.
C	Output (observation) matrix.
x_k	State vector.
A_i	Auto-Regressive coefficient matrix.
B_i	Moving Average coefficient matrix.

1 INTRODUCTION

The system identification task of the BRITE-EURAM project SIMCES (System Identification to Monitor Civil Engineering Structures) consists of extracting the dynamic characteristics of bridges and other civil engineering structures from vibration data. These dynamic characteristics serve as input to model updating and damage assessment techniques. Different types of bridge vibration tests exist. The major difference of these techniques is the way the excitation is applied. One way could be to excite the bridge with a heavy shaker or a drop weight, whereas another could be to use ambient excitation (wind, traffic, waves...). This ladder method has the advantage of being inexpensive since no equipment is needed to excite the bridge. Also by using this technique the service state of the structure does not have to be interrupted.

In this paper, as well as in the SIMCES project, the attention is focused on system identification techniques, which can deal with the ambient response case. The intention is to make a comparison of four different system identification methods. The methods are the frequency domain peak-picking (PP) method, the polyreference LSCE (LSCE) method, a stochastic subspace identification technique for estimation of state space systems (SSI), and the prediction error method (PEM) applied to Auto-Regressive Moving Average Vector (ARMAV) models.

There are several reasons why a comparison of different system identification techniques on operational data cannot be objective. First of all, there is the lack of a reference system, which means that the methods can only be compared relative to one another. The next problem is what to compare. This is a highly subjective choice that depends on the actual application. Some would claim that computational time is the most important parameter while others might emphasize the accuracy of e.g. estimated modal parameters instead. Some are only interested in e.g. the natural frequencies and damping ratios, while others like to have a high resolution estimate of the mode shapes. In the modal analysis community the use of many sensors has for many years made the users emphasize the computationally fast techniques for system identification. However, in recent years, users and modal software companies have drawn their attention towards techniques that are perhaps more time consuming but which can provide more accurate results. At the same time techniques have been developed for optimizing the sensor positioning in order to reduce the number of required sensors. Combining this with the increasing speed of computers, the issue of the computational time is perhaps not so important any more. Therefore, in this paper, emphasis is put on the assessment of the quality of the estimated modal parameters.

The test scenario in this paper involves a large number of sensors divided into several setups, and a large amount of measured data. This implies that the system identification techniques in this paper

are judged in terms of their ability to handle a large number of sensors and data points. It also implies, that all the techniques have data enough to make it possible to assess their asymptotic properties. Due to the lack of a reference system the comparison will not result in the election of a winner, but discuss the strong and weak sides of the different techniques. The comparison will be based on the estimated natural frequencies, damping ratios and mode shapes (Visual inspection and the Modal Assurance Criterion).

The theory behind the four different methods are briefly reviewed in the chapter 2. In chapter 3, the test structure, the Swiss Z24 highway bridge, as well as the test procedure and the practical aspects of using the four different methods, are presented. Chapter 4 presents the results, and in chapter 5 conclusions are made.

2 APPLIED IDENTIFICATION TECHNIQUES

2.1 *Peak-Picking*

A fast method to estimate the modal parameters of a structure based on output-only measurements is the rather simple peak-picking method. The method is widely used and one practical implementation of the method was realized by Felber, see Felber [1]. In this implementation the natural frequencies are determined as the peaks of the Averaged Normalized Power-Spectral Densities (ANPSDs). The ANPSDs are basically obtained by converting the measured data to the frequency domain by a Discrete Fourier Transform (DFT). The coherence function computed for two simultaneously recorded output signals has values close to one at the natural frequencies, see Bendat et al. [2]. This fact also helps to decide which frequencies can be considered natural. The components of the mode shapes are determined by the values of the *transfer functions* at the natural frequencies. Note that in the context of ambient testing, *transfer function* does not mean the ratio of response over force, but rather the ratio of response measured by a roving sensor over response measured by a reference sensor. So every transfer function yields a mode shape component relative to the reference sensor. It is assumed that the dynamic response at resonance is only determined by one mode. The validity of this assumption increases as the modes are better separated and as the damping is lower. The method has been used successfully at EMPA for a large amount of structures, see Felber et al. [3].

2.2 *Polyreference LSCE applied to Auto- and Cross-Correlation Functions*

On the assumption that the system is excited by stationary white noise it has been shown that correlation functions between the response signals can be expressed as a sum of decaying sinusoids, see James et al. [4]. Each decaying sinusoid has a damped natural frequency and damping ratio that is identical to that of a corresponding structural mode. Consequently, the classical modal parameter estimation techniques using impulse response functions as input like Polyreference LSCE, Eigensystem Realization Algorithm (ERA) and Ibrahim Time Domain are also appropriate for extracting the modal parameters from response-only data measured under operational conditions. This technique is also referred to as NExT, standing for Natural Excitation Technique, see James et al. [4]. In this paper the discussion will be limited to polyreference LSCE.

The correlation functions between the outputs and a set of outputs serving as references are defined as:

$$R_k = E[y_{k+m}\, y_{ref,m}^T] \in \mathbb{R}^{l \times l_{ref}} \tag{1}$$

$y_k \in \mathbb{R}^{l \times 1}$ is the output vector containing l channels, $y_{ref,k} \in \mathbb{R}^{l_{ref} \times 1}$ is a subset of y_k containing only the l_{ref} references, and $E[\bullet]$ denotes the expected value. The correlation functions can be estimated by replacing the expected value operator in (1) by a summation over the available measurements. Another way to estimate the correlation functions can be implemented by taking the inverse DFT of power- and cross-spectral densities which are calculated on the basis of the DFT and segment averaging. Although this method is faster than performing the calculation in the time domain, it is less accurate as it suffers from leakage.

The polyreference LSCE yields global estimates of the poles and the modal reference factors [5]. Mathematically, the polyreference LSCE will decompose the correlation functions as a sum of decaying sinusoids:

$$R_k = \sum_{r=1}^{n_p} \left\{ \psi_r\, \lambda_r^k\, L_r^T + \psi_r^*\, \lambda_r^{*k}\, L_r^{*T} \right\} \tag{2}$$

where n_p is the number of poles; $\psi_r \in \mathbb{C}^{l \times 1}$ is the r mode shape; $\lambda_r = e^{\mu_r \Delta t}$ is the r complex discrete system pole (related to the continuous system pole μ_r and the sample time Δt); $L_r \in \mathbb{C}^{l_{ref} \times 1}$ is a vector of multipliers which are constant for all response stations for the r mode. Note that in conventional modal analysis, these constant multipliers are the modal participation factors. In case of output-only modal analysis, they will be further referred to as the modal reference factors. It can be proved that if the correlation data can be described by (2), it can also be described by the following model:

$$R_k I + R_{k-1} F_1 + \ldots + R_{k-i} F_i = 0 \tag{3}$$

if the following conditions are fulfilled:

$$L_r^T \left(\lambda_r^k I + \lambda_r^{k-1} F_1 + \ldots + \lambda_r^{k-i} F_i \right) = 0 \tag{4}$$

$$l_{ref} \times i \geq 2 n_p \tag{5}$$

Equation (3) represents a coupled set of l_{ref} finite difference equations with constant matrix coefficients ($F_1, \ldots, F_i \in \mathbb{R}^{l_{ref} \times l_{ref}}$). The condition expressed by (4) states that the terms λ_r, L_r^T are characteristic solutions of this system of finite difference equations. As (3) is a superposition of $2n_p$ of such terms, it is essential that the condition given by (5) is fulfilled.

Polyreference LSCE essentially comes down to estimating the matrix coefficient $F_1, \ldots, F_i$. Once these are known, (4) can be reformulated into a generalized eigenvalue problem resulting into $l_{ref} \times i$ eigenvalues λ_r, yielding estimates for the system poles μ_r and the corresponding left eigenvectors L_r^T. Equations similar to (3) can be formulated for all possible correlations R_k. The obtained over-determined set of equations can than be solved in a least squares sense to yield the matrix coefficients $F_1, \ldots, F_i$. The order i of the finite difference equation is related to the number of modes in the data. Selection of the model order can be done by observing the least-squares error as a function of the assumed order. As an order is reached such that the model can describe as many modes as present in the data, the error should drop significantly. In practice, stabilisation diagrams are typically used to determine the optimal number of modes. Frequencies, damping values and modal reference factors calculated from models of consecutive order are compared. The selection of outputs which function as references for the estimation of the empirical correlations (1) has to be made in such a way that they contain all of the relevant modal information. In fact,

the selection of output-reference channels is similar to choosing the input-reference locations in a traditional modal test.

Contrary to the stochastic subspace and ARMAV methods (cf. the next two sections), the polyreference LSCE does not yield the mode shapes. So, a second step is needed to extract the mode shapes using the identified modal frequencies and modal damping ratios. This can be done either by fitting the correlation functions in the time domain or by fitting the power- and cross-spectral densities in the frequency domain, see Hermans et al. [6]. The fitting step offers the advantage that not all responses should be included in the time-domain parameter extraction scheme and that consequently, mode shapes of a large number of response stations can be easily processed by consecutively fitting the data. Additionally, it provides a graphical quality check by overlaying the test data with the synthesized data.

2.3 *Stochastic Subspace Identification*

Unlike the two previous methods the stochastic subspace identification method directly works with the recorded time signals. The peak-picking method requires frequency domain data while the polyreference LSCE method needs the correlation functions between time signals. It is beyond the scope of this paper to explain in full detail the stochastic subspace identification method. The interested reader is referred to Van Overschee et al. [7,8], Kirkegaard et al. [9] and Peeters et al. [10,11] for the theoretical background and applications in civil engineering. Here only the main ideas behind the method are given. The method assumes that the dynamic behaviour of a structure excited by white noise can be described by a stochastic state space model:

$$\begin{aligned} x_{k+1} &= A x_k + w_k \\ y_k &= C x_k + v_k \end{aligned} \tag{6}$$

where $x_k \in \mathbb{R}^{2n_p \times 1}$ is the internal state vector; n_p is the number of poles; $y_k \in \mathbb{R}^{l \times 1}$ is the measurement vector and w_k, v_k are white noise terms representing process noise and measurement noise together with the unknown inputs; $A \in \mathbb{R}^{2n_p \times 2n_p}$ is the state matrix containing the dynamics of the system and $C \in \mathbb{R}^{l \times 2n_p}$ is the output matrix, translating the internal state of the system into observations.

The subspace method then identifies the state space matrices based on the measurements and by using robust numerical techniques such as QR-factorization, Singular Value Decomposition (SVD) and least squares. Roughly, the QR results in a significant data reduction, whereas the SVD is used to reject the noise (assumed to be represented by the higher singular values). Once the mathematical description of the structure (the state space model) is found, it is straightforward to determine the modal parameters (by an eigenvalue decomposition): natural frequencies, damping ratios and mode shapes

2.3 *ARMAV Estimation using a Prediction Error Method*

Just like the stochastic subspace identification method the Prediction Error Method for estimation of ARMAV models works directly with the recorded time signals. A detailed description of the Prediction Error Method is provided in Ljung [12] and Söderström et al. [13], and a comprehensive description of the use of ARMAV models in relation to civil engineering and mechanical applications is found in Andersen [14] and Pandit [15]. It can be shown that the ARMAV model can model the dynamics of a structure subjected to filtered white noise, see Andersen [14]. In other words, the only restrictions are that the structure behaves linearly and is time-invariant, and that the unknown input force can be modelled by a white noise filtered through a linear and time-invariant shaping filter. The definition of the ARMAV model is:

$$\begin{aligned} y_k + A_1 y_{k-1} + \ldots + A_n y_{k-n} &= \\ e_k + B_1 e_{k-1} + \ldots + B_n e_{k-n} & \end{aligned} \tag{7}$$

where $y_k \in \mathbb{R}^{l \times 1}$ is the measurement vector and $e_k \in \mathbb{R}^{l \times 1}$ is a zero-mean white noise vector process. The auto-regressive matrix polynomial is described by the coefficient matrices $A_i \in \mathbb{R}^{l \times l}$. This polynomial models the dynamics of the combined system, i.e. the modes of the structural system combined with the noise modes. The moving average matrix polynomial is described by the coefficient matrices $B_i \in \mathbb{R}^{l \times l}$. This polynomial ensures that the statistical description of the data is optimal. It can be shown that by adding this moving average the covariance function of the predicted output $\hat{y}_k$ of the ARMAV model will be equivalent to the covariance function of y_k, see Andersen et al. [16]. The model order n depends on the number of modes as well as on the dimension of the measurement vector.

The ARMAV model is calibrated to the measured time signals by minimizing the prediction error $y_k - \hat{y}_k$, i.e. the difference between the measured time signals and the predicted output of the ARMAV model. The criterion function V that is minimized is defined as, see Ljung [12] and Andersen et al. [17]:

$$V = \det\left(\frac{1}{N} \sum_{k=1}^{N} \left(y_k - \hat{y}_k\right)\left(y_k - \hat{y}_k\right)^T \right) \tag{8}$$

This criterion function can be shown to correspond to a maximum likelihood if the prediction errors are Gaussian white noise, see Söderström et al. [13]. In this case the criterion provides maximum accuracy [Söderström]. The presence of the moving average makes it necessary to apply a non-linear optimization scheme. This minimization is started by providing an initial ARMAV model. In the present case this model is obtained by a stochastic subspace method, see Andersen [14]. Again, once the optimal ARMAV model is determined by a stabilization diagram, it is straightforward to determine the modal parameters by a modal decomposition.

3 TESTING OF THE Z24 HIGHWAY BRIDGE

The bridge, used as test object to compare the above mentioned system identification methods, is the Z24-bridge overpassing the national highway A1 between Bern and Zürich in Switzerland. It is a prestressed concrete box girder bridge with a main span of 30 m and two side spans of 14 m. The bridge is supported by 4 piers clamped into the girders. The two piers at the abutments are completely embedded in the ramps. The bridge is slightly skew: the axes of the piers are not perpendicular to the longitudinal axis of the bridge (deviation by 13°).

3.1 *Description of the Acquired Data*

In total, 145 points were measured, mainly in the vertical and transverse direction. This amounted to 172 degrees of freedom (DOFs). The same number of channels would have been necessary to measure all the DOFs at the same time. As a maximum of 23 channels were available the testing were divided into 9 setups. In each setup 19 different DOFs on the bridge were measured, along with 4 extra DOFs serving as references (3 in vertical direction and 1 in the transverse direction). These reference stations were measured again in each setup. The data were sampled at a rate of

80 Hz and the analogue anti-aliasing filter had a cut-off frequency at 20 Hz. A total of 65536 samples (13 min, 39.2 sec) wes acquired for each channel and each setup. Figure 1 shows the measurement grid of the bridge.

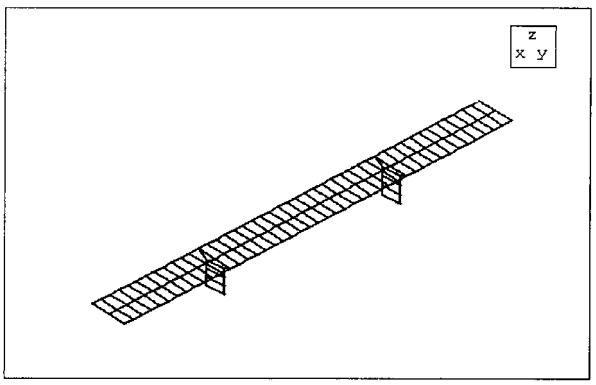

Figure 1: Geometry of the bridge.

An important observation was that the excitation was not the same for each setup. This can be seen from figure 2, showing the power-spectral densities of a fixed reference station for setups 2 to 7.

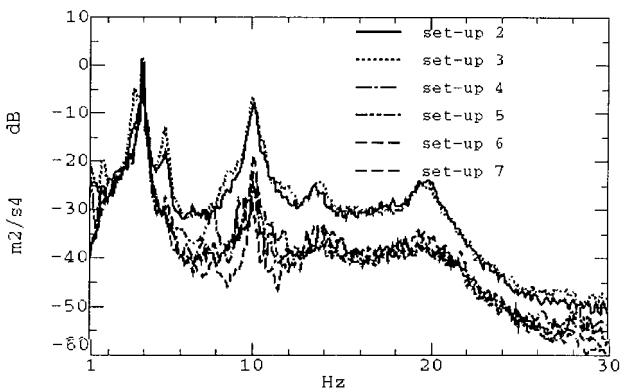

Figure 2: Power-spectral densities of a reference station in vertical direction for setups 2 to 7.

The ambient excitation sources of the bridge were wind and traffic on the highway. All setups were measured between 9 PM and midnight. The test crew of EMPA observed that the wind died off to a probably insignificant level a short time after the beginning of the test. The traffic on the highway seemed to die off after about 9 to 10 PM, picked up again towards 11 PM, and died out close to midnight. More details concerning the bridge test can be found in Krämer et al. [18]

3.2 *Practical Aspects of Using the Different Identification Techniques*

For the peak-picking method, 16 segments of 4096 data points were transformed to the frequency domain and averaged to estimate the power-spectral densities. So all measured data were used in this method. By applying the procedures described in section 2.1, estimates of the natural frequencies and mode shape parts were obtained. Every setup with 23 simultaneously recorded signals yields the mode shape at the corresponding 23 DOFs. The different parts were glued together using one of the reference sensors (the choice of the reference sensor depends on the *nature* of the mode shape).

The polyreference LSCE method was applied to the auto- and cross-correlations of the responses. For each setup, the correlations between all responses and 3 responses in the vertical direction serving as references were calculated using equation (1). The number of estimated time lags equalled 256 which corresponds to a duration of 3.2 sec. The correlation functions were then fed to the LSCE method in order to extract the natural frequencies and damping ratios. As the correlation functions of the different setups were referenced to the same 3 reference stations, they could be combined into one global model, yielding global estimates for the frequency and damping. Stabilisation diagrams showing the stability of the poles as function of increasing model order were used to distinguish the spurious modes from the physical ones. Next to this global analysis, the modal parameters were also separately extracted for each setup and a comparison of the modal estimates was made. As the LSCE method does not yield the mode shapes, an additional step was needed. This was done by fitting the power- and cross-spectral densities between the responses and the selected reference stations in a least squares sense. The power- and cross-spectral densities were estimated on the basis of the DFT and segment-based averaging. The segment size equalled 2048 time points and 50% overlap was used. A Hanning window was used to reduce the leakage effects. As the excitation was different for each setup, the mode shapes were separately identified for each setup and glued together via the 4 reference stations. For setup 5, the power-spectral densities of a few DOFs were difficult to fit, which leads to some irregularities in the animation of the mode shape. Also, for most setups, the fit was poor for frequencies higher than 12 Hz and consequently, the shape of the fifth mode (cf. next section) could not be extracted with high confidence.

For the stochastic subspace method it was not possible to treat all 65536 samples × 23 channels of one setup at once. The computational time and memory needed can increase to an inadmissible level with an increasing number of samples and channels. Therefore the analysis for all setups was limited to a high-quality segment of 4096 samples. If such a segment did not give satisfactory results, another segment was chosen afterwards to perform a new analysis. The number of time lags used in the method were 20; since there were 23 channels, the maximum number of singular values was 460 (20 × 23). Consecutive state space models of dimension 2 to 60 in steps of 2 were identified. From all these state space models, the modal parameters were extracted. Stabilisation diagrams were then used to distinguish the spurious modes from the physical ones. For every setup, seven modes could be identified.

To apply the prediction error method for estimation of ARMAV models, an accurate initial estimate was needed. By supplying an accurate initial estimate the number of iterations needed was kept at a minimum and convergence was ensured. To provide such initial estimates, a subspace technique returning ARMAV models was applied, see Andersen [14]. The modal parameters of interest of the initial ARMAV models were then refined, one mode at a time, by minimizing (8) in modal space, see Brincker et al. [19]. In the subspace estimation the number of time lags used were 30. All available data were used, i.e. up to 65536 samples × 23 channels per setup. The orders of the applied ARMAV models were in the range from n=1 to n=5. Again, due to the differences of the excitation from setup to setup, the mode shapes were separately identified for each setup and glued together via the 4 reference stations.

4 COMPARISON OF MODAL RESULTS

The results of the comparison are presented in this section mode by mode. In the comparison of the mode shapes only the sensors located at the girder are included. These sensors are placed in three rows along the girder, which means that each mode shape can be represented by three curves. These three curves are plotted in the same figure for all four techniques. Below each of these figures the Modal Assurance Criterion between the four techniques is listed in a table. Also listed are the estimated natural frequencies, damping ratios, and standard deviations.

Five modes have been identified by all four methods. The 1st mode is a vertical bending mode. In the 2nd mode, the piers are bending in the transverse direction and the girder is submitted to torsion. The 3rd and 4th modes are both combinations of bending and torsion. The 5th mode is a bending mode with very active side spans compared to the mid-span. For this reason, this mode is not very identifiable at the measurement points of setup 5 (The mid-setup). Two higher-frequency modes have been identified by both SSI and PEM, but they are omitted in the following comparison, since the two other methods have not identified them.

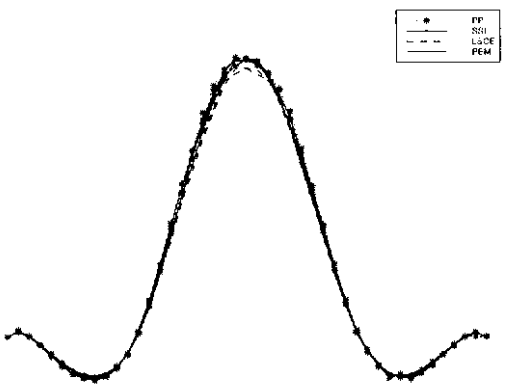

Figure 3: Comparison of the 1st mode shape - All four methods.

	PP	LSCE	SSI	PEM
PP	1	0.9999	0.9999	0.9999
LSCE	0.9996	1	0.9998	0.9998
SSI	0.9999	0.9998	1	1
PEM	0.9999	0.9998	1	1

Table 1: Modal Assurance Criterion of the 1st mode shape.

	f_i [Hz]	ζ_i [%]	σ_{f_i} [Hz]	σ_{ζ_i} [%]
PP	3.96	-	-	-
LSCE	3.95	1.0	0.01	0.2
SSI	3.93	1.1	0.02	0.5
PEM	3.95	1.1	0.01	0.3

Table 2: The natural frequencies and damping ratios of the 1st mode.

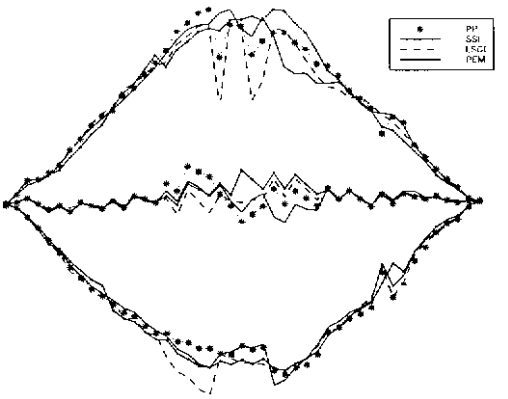

Figure 4: Comparison of the 2nd mode shape -All four methods.

	PP	LSCE	SSI	PEM
PP	1	0.9907	0.9923	0.9945
LSCE	0.9907	1	0.9882	0.9868
SSI	0.9923	0.9882	1	0.9909
PEM	0.9945	0.9868	0.9909	1

Table 3: Modal Assurance Criterion of the 2nd mode shape.

	f_i [Hz]	ζ_i [%]	σ_{f_i} [Hz]	σ_{ζ_i} [%]
PP	5.27	-	-	-
LSCE	5.23	1.8	0.02	0.3
SSI	5.22	1.4	0.02	0.3
PEM	5.24	1.7	0.02	0.5

Table 4: The natural frequencies and damping ratios of the 2nd mode.

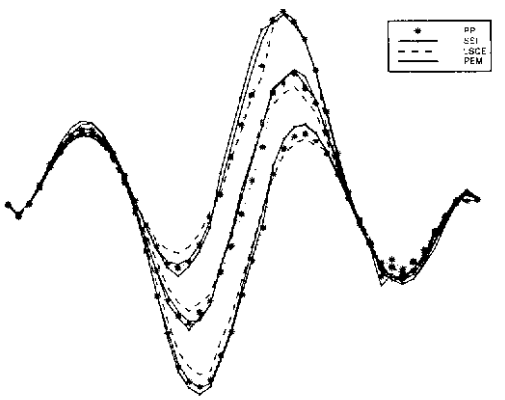

Figure 5: Comparison of the 3rd mode shape - All four methods.

	PP	LSCE	SSI	PEM
PP	1	0.9957	0.9952	0.9962
LSCE	0.9957	1	0.9941	0.9972
SSI	0.9952	0.9941	1	0.9972
PEM	0.9962	0.9972	0.9972	1

Table 5: Modal Assurance Criterion of the 3rd mode shape.

	f_i [Hz]	ζ_i [%]	σ_{f_i} [Hz]	σ_{ζ_i} [%]
PP	10.20	-	-	-
LSCE	10.10	1.4	0.03	0.4
SSI	10.10	1.4	0.04	0.4
PEM	10.09	1.3	0.05	0.5

Table 6: The natural frequencies and damping ratios of the 3rd mode.

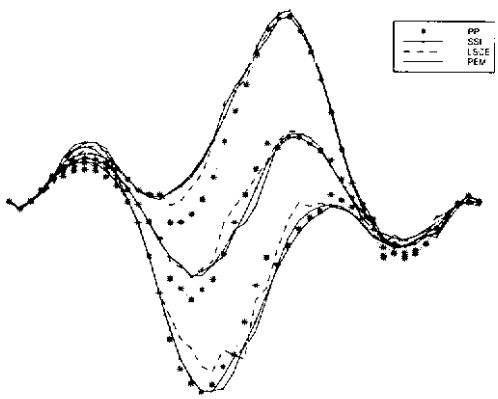

Figure 6: Comparison of the 4th mode shape - All four methods.

	PP	LSCE	SSI	PEM
PP	1	0.9812	0.9856	0.9771
LSCE	0.9812	1	0.9906	0.9913
SSI	0.9856	0.9906	1	0.9956
PEM	0.9771	0.9913	0.9956	1

Table 7: Modal Assurance Criterion of the 4th mode shape.

	f_i [Hz]	ζ_i [%]	σ_{f_i} [Hz]	σ_{ζ_i} [%]
PP	10.82	-	-	-
LSCE	10.73	1.6	0.05	0.5
SSI	10.75	1.2	0.03	0.3
PEM	10.74	1.1	0.05	0.3

Table 8: The natural frequencies and damping ratios of the 4th mode.

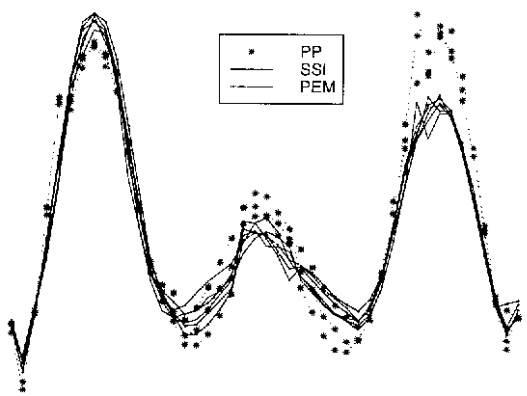

Figure 7: Comparison of the 5th mode shape - All four methods.

	PP	LSCE	SSI	PEM
PP	1	-	0.9749	0.9753
LSCE	-	-	-	-
SSI	0.9749	-	1	0.9944
PEM	0.9753	-	0.9944	1

Table 9: Modal Assurance Criterion of the 5th mode shape.

	f_i [Hz]	ζ_i [%]	σ_{f_i} [Hz]	σ_{ζ_i} [%]
PP	12.8	-	-	-
LSCE	12.8	3.7	0.20	1.0
SSI	12.8	2.1	0.10	0.6
PEM	12.7	3.8	0.05	1.0

Table 10: The natural frequencies and damping ratios of the 5th mode.

In general, all methods seems to agree very well on the natural frequency estimates of the first five modes. Even the damping ratio estimates correspond fairly well for three of the methods. The damping ratios have not been estimated in the peak-picking method, even though a half band-width estimation approach could have been applied. In any case, such an approach would probably not provide comparable estimates.

The mode shape estimates of the two time domain methods, the SSI and the PEM, tend to return similar mode shape estimates. The same can be said about the two other methods, which both estimates the mode shapes in frequency domain. Not surprisingly, it is the first mode that the methods agrees most on. This mode is shown in three dimensions in figure 8.

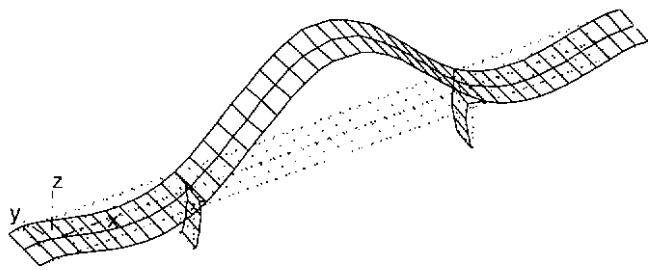

Figure 8: Mode shape of the 1st mode (bending) obtained by the SSI method.

The advantages of the peak-picking method are that it is easy to use and provides fast estimates. However, the damping has not been estimated, and since no parametric model is calibrated, the mode shapes are in fact only operational deflection shapes. In the present case, where all modes are well-separated, deflection shapes seem to approximate the mode shapes well. The advantage of the LSCE method is its ability to identify modal parameters globally, even when data is divided into multiple setups. In the present case, it is seen to provide sound estimates of the natural frequencies and damping ratios that are comparable with the two other time domain methods. Since the mode shapes are estimated in frequency domain they are more comparable with the peak-picking method than the two time domain methods.

The time domain methods have the advantages of operating directly on the measured time signals. However, they are a bit more complicated to use, and more time consuming. Different model orders have to be evaluated in order to determine the optimal one. However, stabilisation diagrams and other model validation techniques can be of aid to the user. The SSI method solves the time and memory problem by reducing the amount of data used in the analysis. The PEM method and the initial subspace estimator of ARMAV models both use all available data. However, due to the high quality data this does not seem to improve the modal parameter estimates significantly.

A final remark could be that peak-picking and other non-parametric methods are fast, easy to use and give reasonable estimates. They should be applied first to give the user a quick look at the dynamic performance. If the user wants more accurate information, as well as

additional information that cannot be provided by non-parametric methods, then he or she can apply one of the more sophisticated time domain methods.

5 CONCLUSIONS

In this paper the performance of four different system identification methods have been compared and discussed. The four methods are the frequency domain based peak-picking methods, the polyreference LSCE method, the stochastic subspace method for estimation of state space systems and the prediction error method for estimation of Auto-Regressive Moving Average Vector models.

The comparison reveals that all methods give reasonable estimates of the natural frequencies and mode shapes. Three of the methods also return comparable estimates of the damping ratios. The advantages of some of the methods are their simplicity and ability to provide fast estimates, whereas the advantages of the other methods are their ability to provide accurate estimates of the modal parameters.

It has not been the intention to elect a winner among the four methods. The preferable method depends solely on the actual application. Also, in practical application several of the methods can complement one another.

ACKNOWLEDGEMENTS

The research has been carried out in the framework of the BRITE-EURAM Programme CT96 0277, SIMCES with a financial contribution by the Commission. Partners in the project are: K.U.Leuven, Aalborg University, EMPA, LMS International, WS Atkins, Sineco, T.U.Graz.

REFERENCES

1. Felber, A.J.: *Development of a hybrid bridge evaluation system.* Ph.D. thesis, Department of Civil Engineering, University of British Columbia, Vancouver, Canada, 1993.
2. Bendat, J.S. & A.G. Piersol: *Engineering applications of correlation and spectral analysis.* 2nd edition, John Wiley & Sons, New York, USA, 1993.
3. Felber, A.J. & R. Cantieni: *Introduction of a new ambient vibration testing system - description of the system and seven bridge tests.* Technical Report 156'521, EMPA, Dübendorf, Switzerland, 1996.
4. James III, G.H., T.G. Carne & J.P. Laufer: *The natural excitation technique (NExT) for modal parameter extraction from operating structures.* Int. J. of Analytical and Experimental Modal Analysis, Vol. 10, No. 4, pp. 260-277, 1995.
5. Brown, D.L. & R.J. Allemang, R. Zimmerman & M. Mergeay: *Parameter estimation techniques for modal analysis*, SAE Paper, No. 790221, 1979.
6. Hermans, L. & H. Van der Auweraer: *On the use of auto- and cross-correlation functions to extract the modal parameters from output-only data.* Proc. of 6th Int. Conf. on Recent Advances in Structural Dynamics, Work in progress paper, Southampton, UK, 1997.
7. Van Overschee, P. & B. De Moor: *Subspace identification for linear systems: theory - implementation - applications.* Kluwer Academic Publishers, Dordrecht, The Netherlands, 1996.
8. Van Overschee, P. & B. De Moor: *Subspace algorithms for the stochastic identification problem.* Proc. of the 30th IEEE Conf. on Decision and Control, pp. 1321-1326, Brighton, UK, 1991.
9. Kirkegaard, P.H. & P. Andersen: *State space identification of civil engineering structures from output measurements.* Proc. of IMAC 15, pp. 889-895, Orlando, Florida, USA, 1997.
10. Peeters, B. & G. De Roeck: *Stochastic subspace system identification of a steel transmitter mast*, Proc. of IMAC 16, pp. 130-136, Santa Barbara, California, USA, 1998.
11. Peeters, B. & G. De Roeck: *The performance of time domain system identification methods applied to operational data.* Proc. of DAMAS '97, Structural Damage Assessment Using Advanced Signal Processing Procedures, pp. 377-386, Sheffield, UK, 1997.
12. Ljung, L.: *System Identification - Theory for the User.* Prentice-Hall, Englewood Cliffs, New Jersey, 1987.
13. Söderström, T. & P. Stoica: *System Identification.* Prentice-Hall, Englewood Cliffs, New Jersey, 1989.
14. Andersen, P.: *Identification of Civil Engineering Structures using Vector ARMA Models.* Ph.D. thesis, Department of Building Technology and Structural Engineering, Aalborg University, Denmark, 1997.
15. Pandit, S.M.: *Modal and Spectrum Analysis: Data Dependent Systems in State Space.* John Wiley & Sons, New York, 1991.
16. Andersen, P., R. Brincker & P.H. Kirkegaard: *Theory of Covariance Equivalent ARMAV Models of Civil Engineering Structures.* Proc. of IMAC 14, pp. 518-524, Dearborn, Michigan, USA, 1996.
17. Andersen, P. & R. Brincker: *Estimation of Modal Parameters and Their Uncertainties.* Proc. of IMAC 17, Orlando, Florida, USA, 1999.
18. Krämer, C. & C.A.M. de Smet: *Brite-EuRam project SIMCES (CT96-0277), task A1: bridge testing, 2nd system identification of Z24 bridge.* Technical Report 168'349/6, EMPA, Dübendorf, Switzerland, 1997.
19. Brincker, R. & P. Andersen: *Vector ARMA Models in Modal Space.* Proc. of IMAC 17, Orlando, Florida, USA, 1999.